1521-009X/50/5/566–575$35.00
DRUG METABOLISM AND DISPOSITION
dx.doi.org/10.1124/dmd.121.000765
Drug Metab Dispos 50:566–575, May 2022

Estimation of Fraction Metabolized by Cytochrome P450 Enzymes Using Long-Term Cocultured Human Hepatocytes[S]

Florian Klammers, Andreas Goetschi, Aynur Ekiciler, Isabelle Walter, Neil Parrott, Stephen Fowler, and Kenichi Umehara

Roche Pharmaceutical Research and Early Development, Roche Innovation Center, Basel, Switzerland

Received November 5, 2021; accepted February 25, 2022

ABSTRACT

Estimation of the fraction of a drug metabolized by individual hepatic CYP enzymes relative to hepatic metabolism (fm,CYP) or total clearance h as been challenging for low turnover compounds due to insufficient resolution of the intrinsic clearance (CLint) measurement in vitro and difficulties in quantifying the formation of low abundance metabolites. To overcome this gap, inhibition of drug depletion or selective metabolite formation for 7 marker CYP substrates was investigated using chemical inhibitors and a micropatterned hepatocyte coculture system (HepatoPac). The use of 3 μM itraconazole was successfully validated for estimation of fm,CYP3A4 by demonstration of fm values within a 2-fold of in vivo estimates for 10 out of 13 CYP3A4 substrates in a reference set of marketed drugs. Other CYP3A4 inhibitors (ketoconazole and posaconazole) were not optimal for estimation of fm,CYP3A4 for low turnover compounds due to their high CLint. The current study also demonstrated that selective inhibition sufficient for fm calculation was achieved by inhibitors of CYP1A2 (20 μM furafylline), CYP2C8 (40 μM montelukast), CYP2C9 (40 μM sulfaphenazole), CYP2C19 [3 μM (-)N-3-benzyl-phenobarbital], and CYP2D6 (5 μM quinidine). Good estimation of fm,CYP2B6 was not possible in this study due to the poor selectivity of the tested inhibitor (20 μM ticlopidine). The approach verified in this study can result in an improved fm estimation that is aligned with the regulatory agencies' guidance and can support a victim drug-drug interaction risk assessment strategy for low clearance discovery and development drug candidates.

SIGNIFICANCE STATEMENT

Successful qualification of a chemical inhibition assay for estimation of fraction metabolized requires chemical inhibitors that retain sufficient unbound concentrations over time in the incubates. The current cocultured hepatocyte assay enabled estimation of fraction metabolized, especially by CYP3A4, during the drug discovery phase where metabolite quantification methods may not be available. The method enables the assessment of pharmacokinetic variability and victim drug-drug interaction risks due to enzyme polymorphism or inhibition/induction with more confidence, especially for low clearance drug candidates.

Introduction

Determination of the fraction metabolized by CYP enzymes relative to total hepatic metabolism (fm,CYP), or total clearance (fCL,CYP), is important to understand the pharmacokinetic (PK) variability and victim drug-drug interaction (DDI) potential of a drug (Bohnert et al., 2016). fCL,CYP values determined in vitro for a molecule can be confirmed by running clinical DDI studies, which measure the change of pharmacokinetics when coadministered with specific CYP enzyme modulators. For example, ibrutinib, developed for treating B-lymphocyte cell malignancies, was proven to have fCL by CYP3A4 of > 0.95 when the potent and selective CYP3A4 inhibitor ketoconazole increased the oral area under the curve (AUC) by 24-fold, whereas the CYP3A inducer rifampicin decreased the oral AUC by 10-fold in clinical DDI studies (de Zwart et al., 2016). To support clinical development plans efficiently it is necessary to conduct victim DDI risk assessment by first estimating fm,CYP in vitro. Siponimod, which reduces the risk of disability progression in patients with multiple sclerosis, is metabolized by CYP2C9, CYP3A4, and other enzymes with respective fm values of 0.79, 0.19, and 0.02 based on in vitro reaction phenotyping (Huth et al., 2019). These fm values, assuming equity with fCL, informed a physiologically based pharmacokinetic (PBPK) model, which was then used to predict PK profiles and victim DDI risks for CYP2C9 genotypes and could later be shown to be in agreement with clinical data.

Different techniques are applied for in vitro CYP enzyme reaction phenotyping in the pharmaceutical industry (Harper and Brassil, 2008). One approach involves determination of metabolic clearance of the test drug with specific chemical inhibitors of the major hepatic CYP enzymes (FDA, 2020). An assay format deploying only one type of biologic material, such as human liver microsomes (HLM) or human hepatocytes, can be a simple and attractive option to predict fm,CYPs for drug candidates at the compound selection stage. However, since

This work was supported by F. Hoffmann-La Roche and no external funding was received.

F.K., A.G., A.E., I.W., N.P., S.F., and K.U. are employees of F. Hoffmann-La Roche. No author has an actual or perceived conflict of interest with the contents of this article.

dx.doi.org/10.1124/dmd.121.000765.

[S] This article has supplemental material available at dmd.aspetjournals.org.

ABBREVIATIONS: AO, aldehyde oxidase; AUC, area under the curve; CLint, intrinsic metabolism clearance; DDI, drug-drug interaction; FCS, fetal calf serum; fm,CYP, fraction metabolized by CYP enzymes in liver; FMO, flavin-containing monooxygenase; fu(inc), unbound fraction in incubates; HLM, human liver microsome; Ki,u, (unbound) inhibition constant; LC-MS, liquid chromatography-mass spectrometry; NBPB, (-)N-3-Benzyl-phenobarbital; P450, cytochrome P450; PAPS, 3′-phosphoadenosine-5′-phosphosulfate; PBPK, physiologically based pharmacokinetic; PK, pharmacokinetic; PPP, 2-phenyl-2-(1-piperidynil) propane; SULT, sulfotransferase; UGT, glucuronosyltransferase.

metabolically stable compounds are increasingly preferred as drug candidates due to longer retention in the body, difficulties in measuring drug turnover or production of small quantities of multiple metabolites may prevent accurate fm estimation. For accurate determination of low metabolic clearance in the absence and presence of selective CYP inhibitors, systems allowing for longer incubation times than primary hepatocytes in suspension (limited to 4–6 hours) are beneficial (Docci et al., 2019). HepatoPac has been shown to provide improved prediction accuracy and precision for hepatic CYP intrinsic metabolic clearance compared with hepatocytes in monoculture (Umehara et al., 2020), and other approaches are also available such as Hurel microliver platform and the relay method (Hultman et al., 2016; Murgasova, 2019). Recently, a method to estimate fm,CYP3A4 by incubating low clearance compounds with high concentrations of erythromycin (a moderate time-dependent CYP3A4 inhibitor) in human HepatoPac was reported (Chan et al., 2020). This was then expanded to estimation of fm,CYP1A2; fm,CYP2C9; fm,CYP2C19; and fm,CYP2D6 by Smith et al. (2021). In addition, the human hepatocyte relay method for CYP enzyme reaction phenotyping has been successfully characterized for metabolically stable compounds (Yang et al., 2016). We wanted to build on these approaches by establishing in vitro to in vivo translation for a wider panel of CYP3A4 substrates and to explore further opportunities for these methodologies to be employed for other CYP enzymes.

In this study, human HepatoPac (multi-donor pooled long-term cocultured hepatocytes) were comprehensively investigated as a tool to estimate fm,CYP by measuring metabolic depletion or selective metabolite formation of probe substrates for CYP1A2, 2B6, 2C8, 2C9, 2C19, 2D6, and 3A4 with coincubation of selective and nonselective CYP inhibitors. A drawback of the chemical inhibition method is that compounds established as specific inhibitors for use in short-term human liver microsomal studies may exhibit some degree of off-target inhibition when used at concentrations needed to ensure inhibition effect over extended incubation periods using human hepatocytes. Therefore, optimization of the inhibitor concentrations suitable for fm,CYP estimation using long-term hepatocyte cultures was performed for all tested CYPs. This was further expanded to investigate the effect of the selective CYP inhibitors on non-CYP enzymes since some evidence of this was previously observed (Kratochwil et al., 2017). Finally, the method was applied to estimate fm,CYP3A4 for 13 drugs, followed by a comparison with data collected from the literature. The verification exercise should enable estimation of fm, especially for CYP3A4, for drug discovery compounds including those with low turnover, leading to early assessment of PK variability and victim DDI risks.

Materials and Methods

Chemicals and Biologic Materials. 1-Aminobenzotriazole, 17β-estradiol, carbazeran, bupropion, buspirone, dextromethorphan, diclofenac, furafylline, 4-hydroxymephenytoin, ketoconazole, nifedipine, prednisolone, quinidine, sulfaphenazole, ticlopidine, tienilic acid, tolbutamide, and zidovudine were purchased from Sigma-Aldrich (St. Louis, MO). *S*-Mephenytoin, posaconazole, 2-phenyl-2-(1-piperidynil) propane (PPP), and repaglinide were obtained from Toronto Research Chemicals (Toronto, Canada). Atorvastatin, benzydamine, and rosuvastatin were purchased from ChemPacific (Baltimore, MD) and Honeywell Research Chemicals (Charlotte, NC), respectively. Montelukast, simvastatin, and tacrine were purchased from Cayman, LKT Laboratories (St. Paul, MN), respectively. Itraconazole was purchased from Spectrum chemical (Wellingborough, UK). (-)N-3-Benzyl-phenobarbital (NBPB) was purchased from CYPEX (Dundee, UK). Alectinib, alprazolam, idasanutlin, midazolam, mefloquine, triazolam, troglitazone, zolpidem, zopiclone, and oxazepam [as internal standard for liquid chromatography-mass spectrometry (LC-MS/MS) analysis] were synthesized at F. Hoffmann-La Roche Ltd. (Basel, Switzerland). Acetonitrile and PBS were obtained from Biosolve Chimie (Dieuze, France) and Thermo Fisher Scientific (Waltham, MA), respectively. DMSO (Sigma-Aldrich) was used to prepare stock solutions of the test drugs, resulting in the designated DMSO concentrations (%, v/v) in the final incubation samples.

Human liver cytosols (150-donor pool; mixed gender), recombinant UGT1A1, UGT2B7, and FMO3 were obtained from Corning Inc (One Riverfront Plaza Corning, NY). Ready-to-use Human HepatoPac cultures (long-term hepatocyte cocultures; mixed, $n = 5$ for male and $n = 5$ for female) and stromal mouse fibroblasts (lots/donors: 8305/YFA and 9177/ACR; pooled) with the plates for incubations, application medium, and maintenance medium were acquired from BioIVT.

Metabolism by Human Cocultured Hepatocytes in the Absence of Chemical Inhibitors of P450s. After delivery of the cell culture plates, the medium will be exchanged with maintenance medium and kept at 37°C with 10% CO_2 until the experiment starts. Before the experiment starts, the cells were preincubated with application medium at 37°C and 5% CO_2 for at least 2 hours. Incubations for the test compounds (0.1, 1, or 3 μM; 0.1% v/v DMSO; except for 40 μM *S*-mephenytoin and 10 μM idasanutlin) were performed in 96-well plates containing either a coculture of adherent hepatocytes with mouse fibroblast control cells or control cells alone (5% CO_2 atmosphere and 37°C). HepatoPac kits contained 5000 human hepatocytes per well in a 96-well plate. At defined time points (2, 18, 26, 48, 72, and 96 hours), whole wells were quenched with two-volumes of ice-cold acetonitrile containing an internal standard. Samples were then centrifuged appropriately and the supernatant analyzed by LC-MS/MS.

Measured concentrations were plotted against incubation time (min) and a linear fit made to the natural logarithm transformed data with emphasis upon the initial rate of compound disappearance, except for incubating with *S*-mephenytoin where formation rates of the selective metabolite (4'-hydroxymephenytoin) were monitored. This calculation was performed for samples prepared from HepatoPac and fibroblast control cells (stromal cells). The slope of the fit was then used to calculate the apparent intrinsic clearance:

$$CLint, app\ (\mu L/min/mg\ protein) = [slope\ of\ depletion\ or\ metabolite\ formation\ (min^{-1}) \times 1000] / protein\ concentration\ (mg\ protein/mL) \quad (1)$$

The apparent intrinsic clearance was corrected for fibroblast metabolism. Each well in HepatoPac plates has 75% surface area as fibroblasts and 25% surface area as hepatocytes (Khetani and Bhatia, 2008; Chan et al., 2019). The in vitro intrinsic clearance determined from the fibroblast lysate according to eq. 1 were multiplied by 0.75 and then subtracted from the respective value determined in HepatoPac plates to exclude metabolic clearance by fibroblasts. Hence, the hepatocyte-specific intrinsic clearance (CLint) was calculated using eq. 2:

$$CLint\ (\mu L/min/mg\ protein) = HepatoPac\ CLint, app\ (\mu L/min/mg\ protein) - (0.75 \times Fibroblasts\ (stromal\ cells)\ CLint\ (\mu L/min/mg\ protein)) \quad (2)$$

It was assumed that intrinsic clearance values in the current in vitro assays were measured under linear conditions: substrate concentration (S) < Km and therefore fm estimation unaffected by any small variations in drug concentration, e.g., due to protein binding or change of drug concentration with time. Based on the high quality and reproducibility of the data for depletion slopes previously measured in our laboratory for a large number of test substances in human HepatoPac cells (Docci et al., 2019), which was irrespective of the clearance classification (low to high from 0.2 to 100 μl/min/mg protein), incubations could be efficiently carried out on a single occasion using metabolism time-course profiles made up of 6 independently measured incubation wells. There was high experiment to experiment consistency as illustrated by our quinidine CLint data collected over many experiments (Supplemental Fig. 2). HepatoPac cells were prepared from pooled donor livers throughout the study.

Assessment of Metabolic Depletion of Chemical Inhibitors of CYP3A4. For assay validation, the retention of the chemical inhibitors in the incubate medium was assessed via determinations of their intrinsic hepatic unbound clearance (CLint,u) (eq. 3):

$$CLint,u\ (\mu L/min/mg\ protein) = CLint\ (\mu L/min/mg\ protein)/fu(inc) \quad (3)$$

where fu(inc) is the unbound fraction in incubates. Furthermore, it was assumed that the unbound concentration in the medium represents the intracellular hepatocyte concentration (i.e. no active transport was also assumed). Then a one-compartment model was applied (software: Phoenix 64; Certara Inc., Princeton, NJ) using the measured total CLint values for the four CYP3A4 inhibitors to simulate unbound concentrations for 4 days after single dosing at total concentrations of 0.3, 1, and 3 μM. The fu(inc) in the samples supplemented with 10% fetal calf serum (FCS) were 0.23 for ketoconazole, 0.13 for ritonavir, 0.01 for itraconazole, and 0.17 for posaconazole. These were estimated with the dilution method (Schumacher et al., 2001) using reported plasma unbound fractions: ketoconazole: 0.029 (SimCYP Version 18), ritonavir: 0.015 (SimCYP Version 18), itraconazole: 0.0015 (Chen et al, 2019b), and posaconazole: 0.02 (Cristofoletti et al., 2017). The minimum achieved ratio of simulated unbound inhibitor concentrations to the respective inhibition constants was also calculated.

Inhibition of P450-Mediated Metabolism by Chemical Inhibitors. The chemical inhibitors of CYPs were used at the following concentrations: furafylline (CYP1A2, 20 μM), PPP (25 and/or 100 μM; CYP2B6), ticlopidine (20 μM; CYP2B6), montelukast (40 μM; CYP2C8), sulfaphenazole (40 or 100 μM; CYP2C9), NBPB (3 μM; CYP2C19), quinidine (5 μM; CYP2D6), ketoconazole (0.1, 1, or 3 μM; CYP3A4), itraconazole (0.1, 1, or 3 μM; CYP3A4), posaconazole (0.1, 1, or 3 μM; CYP3A4), ritonavir (0.1, 1, or 3 μM; CYP3A4), and aminobenzotriazole (1 mM; nonselective CYP inhibitor) supplemented with tienilic acid (15 μM; CYP2C9). The reactions were started by adding the substrate and inhibitor solutions, terminated by addition of two volumes of ice-cold acetonitrile containing an internal standard for LC-MS measurement. Incubations served as vehicle controls representing maximal substrate metabolism under the conditions used. The final concentration of the organic solvent in the incubation mixtures was equal to 0.1%. All incubations were carried out in $n = 1$ or 2.

Inhibitory Effects of the Chemical Inhibitors on Non-P450 Enzyme Activities in the Liver. The effects of chemical inhibitors [furafylline (20 μM), PPP (100 μM), montelukast (1 or 40 μM), sulfaphnazole (100 μM), NBPB (3 μM), quinidine (5 μM), and itraconazole (0.1 or 3 μM)] on direct glucuronidation of 17β-estradiol (10 μM, a substrate of UGT1A1) and zidovudine (10 μM, a substrate of UGT2B7) were evaluated using the human recombinant enzymes pretreated with 10 μg/ml alamethicin. The oxidative metabolism of 10 μM benzydamine by human recombinant FMO3 were also measured in the presence of the chemical inhibitors of CYPs. Individual enzyme preparations (0.5 mg/ml for UGT1A1, UGT2B7, and FMO3) were preincubated with a designated substrate in 100 mM Tris-HCl buffer (pH 7.5) or 100 mM sodium phosphate buffer (pH 7.4), with 5 mM magnecium chloride in the absence and presence of inhibitors for 30 minutes at 37°C. The reactions were started by adding uridine 5′-diphosphoglucuronic acid (4.5 mM) for glucuronosyltransferase (UGTs) and reduced β-nicotinamide adenine dinucleotide 2′-phosphate solution (NADPH, 1 mM) for FMO3, and then terminated after 2, 5, 10, 15, 30, and 45 minutes by addition of two volumes of ice-cold acetonitrile containing an internal standard for LC-MS measurement. The final concentration of the organic solvent DMSO in the incubation mixtures was 0.1%. All incubations were carried out in $n = 1$ or 2.

Incubations of 1 μM carbazeran [a substrate of aldehyde oxidase (AO)] and 1 μM troglitazone [a substrate of sulfotransferase (SULT)] with human liver cytosols (0.5 mg protein/ml) were performed in 96-well plates in the presence of the chemical inhibitors of CYPs stated as above. The reactions were started by adding 3′-phosphoadenosine-5′-phosphosulfate (PAPS, 5 mM) for SULT reactions, and then terminated after 2, 5, 10, 15, 30, and 45 minutes. The final concentration of the organic solvent DMSO in the incubation mixtures was 0.1%. All incubations were carried out in $n = 1$ or 2.

All absolute activities for metabolism by UGT1A1, UGT2B7, FMO3, AO, and SULTs in the absence and presence of the chemical inhibitors were converted into relative activities by defining the enzymatic activity without addition of inhibitor as 100% using Microsoft Excel Version 2016 (Microsoft Corporation, Redmond, WA).

LC-MS/MS Analysis. The high-performance liquid chromatography system consisted of LC-30AD pumps, a CBM-20A controller, a CTO-20AC oven, a DGU-20A5R degasser from Shimadzu (Kyoto, Japan), and a HTS CTC PAL auto-sampler (CTC Analytics AG; Zwingen, Switzerland). Sample solutions (5 μl) were injected into the analytical column heated to 60°C [Ascentis Express C18; 2 cm × 2.1 mm, particle size: 2.7 μm; and Supelco, Triart or YMC (for troglitazone) C18 plus; 33 × 2.1 mm, particle size: 3 μm]. To elute the compounds, the following mobile phases used were: A – Water + formic acid 0.1% or formic acid 0.5% (v/v) for troglitazone; and B – acetonitrile + formic acid 0.1% or acetonitrile for troglitazone. A high pressure linear gradient from 0% to 95% B in 40 seconds was applied at a flow rate of 600 μl/min. MS detection with multiple reaction monitoring was operated in the positive ion mode with an API6500 mass spectrometer equipped with a TurboIonSpray source (IonSpray Voltage 5,500V; Sciex, Framingham, MA). Analyst 1.6.3 software (Sciex) was used for data processing using linear regression with $1/x^2$ weighting on peak area ratio. The precision and accuracy of linear regression of the standard curve samples was between 80% and 120%.

Calculation of fm,P450 or fCL,P450. The CLint (given in μl/min/mg protein) of the test drug in human HepatoPac was calculated by dividing decrease rate of the parent drug or the formation rate of the oxidation product by the initial substrate concentration and the protein concentration (eqs. 1 and 2). The fm,CYP or fCL,CYP was determined as [1 – (ratio of CLint in the presence versus absence of the chemical inhibitor)] using Microsoft Excel Version 2016 (Microsoft Corporation, Redmond, WA).

Static Calculation of AUC Changes in the Absence and Presence of Strong CYP3A4 Inhibition Effects. The systemic exposure change of the 13 reference drugs with comedications of a strong CYP3A4 inhibitor was calculated using measured and observed fm,CYP3A4 values in this study according to eq. 4:

$$AUCR = \frac{1}{1 - fm,CYP3A4} \quad (4)$$

where AUCR is an AUC ratio of a victim drug in the presence and absence of coadministration of a perpetrator drug. These extrapolated results are due to the complete inhibition effect on the hepatic metabolism and represent the situation in a preclinical research and development setting where further information related to oral bioavailability and nonmetabolic clearance pathways is not yet available. Therefore, only the predicted categories of victim DDI risks based on the AUCR values were reported in this study according to FDA (2020): no (AUCR < 1.25), weak (1.25 ≤ AUCR < 2), moderate (2 ≤ AUCR < 5), and strong (5 ≤ AUCR).

Results

Selection of a CYP3A4 Inhibitor to Estimate fm,CYP3A4. Depletion of CYP3A4 inhibitors (ketoconazole, itraconazole, ritonavir, and posaconazole) over 4 days of incubation time in long-term cocultured hepatocytes is shown in Fig. 1, with in vitro metabolic clearance (CLint) values at 1 μM of 24.1, 6.50, 3.50, and 6.50 μl/min/mg determined, respectively. Effects of the inhibitors at 0.3, 1, and 3 μM on the metabolism of midazolam (1 μM) are summarized in Table 1.

Estimated fm,CYP3A4 of midazolam with coincubation of itraconazole at 3 μM (0.88) was comparable to a reported fm,CYP3A4 of ~0.9 in HLM (Njuguna et al., 2016). This magnitude of inhibition was not achieved at a lower concentration of itraconazole (0.3 μM). Both ketoconazole and midazolam showed moderate to high metabolic CLint: 24.1 and 33.4 μl/min/mg, respectively (Table 1). Although a strong inhibition was demonstrated by ketoconazole over the first day of incubation (e.g., with midazolam as victim drug) this might not be sufficiently sustained to be suitable for coincubation with low turnover compounds performed over several days. Ritonavir also showed strong CYP3A4 inhibition and might be used as an alternative to 3 μM itraconazole for fm,CYP3A4 estimation in human long-term cocultured hepatocytes, in alignment with a previous report (Greenblatt and Harmatz, 2015). Posaconazole provided a moderate inhibition of CYP3A4,

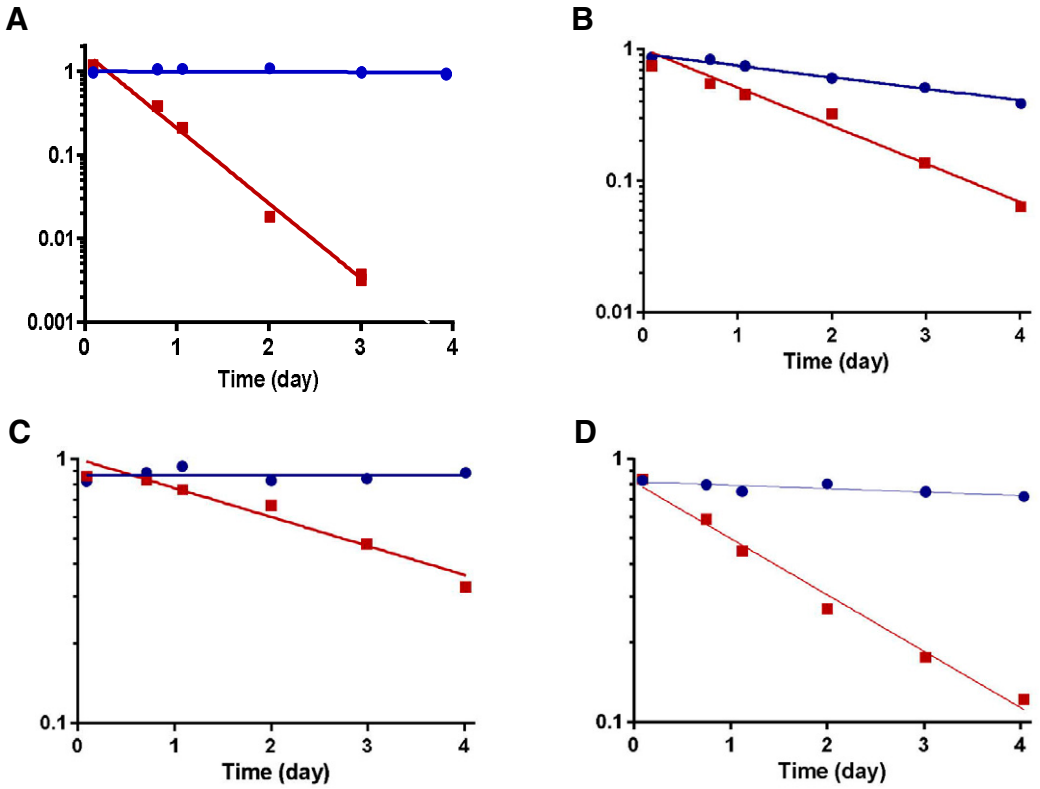

Fig. 1. Depletion of CYP3A4 inhibitors over time in human long-term cocultured hepatocytes. Ketoconazole (A), itraconazole (B), ritonavir (C), and posaconazole (D) at 1 μM were administered at time 0 on day 1, and then incubated for 4 days in human hepatocytes cocultured with mouse stromal cells (closed squares), and in mouse stromal cells (negative controls; closed circles). The compound concentrations on y-axis (μM) in semi-logarithmic scale were plotted against the incubation time on x-axis (day). The depletion profiles of the compounds over time (mean, n = 2) were approximated according to linear regression analysis, resulting in calculation of the CLint values. Contribution of stromal cells to the total metabolic clearance was subtracted from the degradation observed in the cocultured hepatocytes.

possibly due to incomplete inhibition at the tested concentrations, leading to calculation of a lower fm,CYP3A4 of midazolam (0.59–0.73).

Hence, the use of 3 μM itraconazole was selected to estimate fm,CYP3A4 in the current reaction phenotyping study.

Metabolism of the Probe P450 Substrates in the Presence of Chemical Inhibitors. The well known inhibitors furafylline (20 μM; CYP1A2), PPP (25 and/or 100 μM; CYP2B6), ticlopidine (20 μM; CYP2B6), montelukast (40 μM; CYP2C8), sulfaphenazole (40 μM; CYP2C9), NBPB (3 μM; CYP2C19), quinidine (5 μM; CYP2D6), and itraconazole (3 μM; CYP3A4) inhibited their respective substrate depletion in human long-term cocultured hepatocytes by up to 93%, 0%, 41%, 82%, 37%, 83%, 88%, and 83%, respectively (Fig. 2; Table 2).

PPP, a nominal CYP2B6 inhibitor, showed no inhibition of CYP2B6 at 25 and 100 μM and another CYP2B6 inhibitor, ticlopidine, showed only 41% inhibition of total depletion of bupropion and inhibited the turnover of substrates selective for other enzymes by > 30%, namely tacrine (CYP1A2, 84%), diclofenac (CYP2C9, 61%), and dextromethorphan (CYP2D6, 54%). Such off-target activity was also observed for other

TABLE 1

Metabolic clearance of midazolam with and without coincubation of CYP3A4 inhibitors in human long-term cocultured hepatocytes

Midazolam CLint at 1 μM in the absence or presence of CYP3A4 inhibitors at the designated initial concentrations in human cocultured hepatocytes was measured as the midazolam depletion rate over a 4-day incubation period. Midazolam and the inhibitors were applied at time 0 on day 1 and there were no further applications. The fm,CYP3A4 values of midazolam under each inhibition assay condition were calculated as (1 – a ratio of midazolam CLint with and without CYP3A4 inhibition). CLint values the mean of duplicates. CI95 represents the respective CLint with 95% interval for the fitting estimate of CLint based on the midazolam depletion profiles over time according to linear regression analysis.

	CYP3A4 Inhibitor Concentration (μM)	Midazolam CLint (μl/min/mg)	Midazolam fm,CYP3A4
Control (Midazolam Alone)	NA	35.8 (CI95: 1.0)	NA
+Itraconazole	0.3	10.2 (1.1)	0.72
	1	3.5 (0.8)	0.90
	3	4.4 (0.2)	0.88
+Ketoconazole	0.3	14.3 (3.7)	0.60
	1	6.8 (2.1)	0.81
	3	6.0 (1.0)	0.83
+Ritonavir	0.3	3.8 (5.0)	0.89
	1	5.3 (2.6)	0.85
	3	Not tested	NA
+Posaconazole	0.3	14.5 (1.3)	0.59
	1	9.6 (0.7)	0.73
	3	13.2 (3.5)	0.63

NA, not applicable.

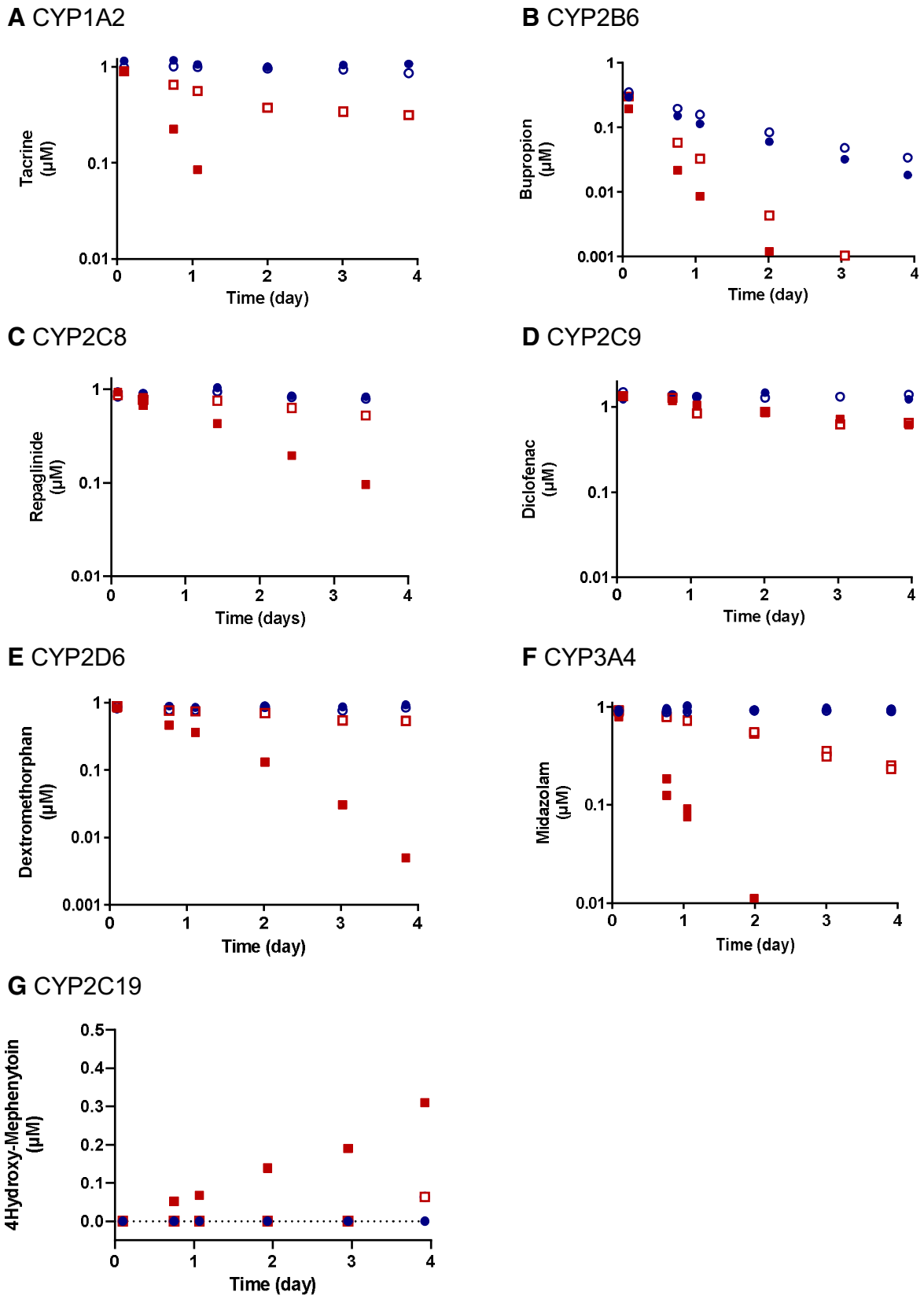

Fig. 2. Probe CYP substrate or specific metabolite concentrations over time in the absence and presence of the selective CYP inhibitors in human long-term cocultured hepatocytes. The effects of selective CYP inhibitors furafylline (CYP1A2, 20 μM), ticlopidine (20 μM; CYP2B6), montelukast (40 μM; CYP2C8), sulfaphenazole (40 μM; CYP2C9), NBPB (3 μM; CYP2C19), quinidine (5 μM; CYP2D6), and itraconazole (3 μM; CYP3A4) on probe CYP marker activities over 4-days incubation time in human cocultured hepatocytes was illustrated: (A) tacrine (CYP1A2), (B) bupropion (CYP2B6), (C) repaglinide (CYP2C8), (D) diclofenac (CYP2C9), (E) dextromethorphan (CYP2D6), and (F) midazolam (CYP3A4) and (G) 4'-hydroxymephenytoin formation at 40 μM *S*-mephenytoin (CYP2C19), respectively. The probe substrate concentration was 1 μM; otherwise noted as above. The probe CYP substrates and inhibitors were applied at time 0 on day 1, and no further multiple

TABLE 2

Effects of chemical inhibitors on CYP substrate turnover in human long-term cocultured hepatocytes

In vitro intrinsic metabolic clearance (CLint) values were determined by measuring linear depletion rates of the parent drugs at 1 μM after incubating with human cocultured hepatocytes for 4 days, except for CYP2C19 (4'-hydroxymephenytoin formation rates at 40 μM S-mephenytoin). Fractions inhibited were calculated as [1 – (ratio of CLint in the presence versus absence of the chemical inhibitor)]. The data represent mean values of duplicate experiments.

		Substrate Selectivity of the CYP Inhibitors in Human Cocultured Hepatocytes (Shown as Fraction Inhibited)						
	Chemical Inhibitor (Initial Concentration at Time 0)	CYP1A2 (tacrine)	CYP2B6 (bupropion)	CYP2C8 (repaglinide)	CYP2C9 (diclofenac)	CYP2C19 (*S*-mephenytoin)	CYP2D6 (dextromethorphan)	CYP3A4 (midazolam)
CYP1A2	furafylline (20 μM)	0.93	0.00	0.05	0.00	0.00	0.48	0.00
CYP2B6	PPP (25 μM /100 μM)	0.19/0.00	0.00/0.00	0.00/-	0.04/0.32	0.00/0.25	0.01/0.45	0.01/0.16
	ticlopidine (20 μM)	0.84	0.41	0.00	0.61	0.17	0.54	0.00
CYP2C8	montelukast (40 μM)	0.11	0.00	0.82	0.00	0.00	0.00	0.20
CYP2C9	sulfaphenazole (40 μM)	0.04	0.04	0.11	0.37	0.00	0.00	0.00
CYP2C19	NBPB (3 μM)	0.05	0.25	0.00	0.28	0.83	0.00	0.00
CYP2D6	quinidine (5 μM)	0.07	0.00	0.10	0.18	0.00	0.88	0.00
CYP3A4	Itraconazole (3 μM)	0.34	0.00	0.29	0.18	0.00	0.10	0.83
CYPs	ABZ (1 mM) with tienilic acid (15 μM)	0.92	0.00	0.77	0.51	1.00	0.96	0.83

ABZ, aminobenzotriazole.

CYPs. 20 μM furafylline (a CYP1A2 inhibitor) showed 48% inhibition of CYP2D6 and 100 μM PPP showed 45% inhibition of CYP2D6. Furthermore, 40 μM sulfaphenazole demonstrated only a weak inhibition (37%) of total depletion of diclofenac, a dual substrate of CYP2C9 and UGT2B7 (Table 2), which was lower compared with the inhibition degree of the selective metabolite formation (89%) due to CYP2C9 in HLM supplemented with NADPH (Njuguna et al., 2016). Weak inhibition (34% and 29%, respectively) was seen on the depletion of tacrine (CYP1A2 substrate) and repaglinide (CYP2C8 substrate) with 3 μM itraconazole (Table 2). This represents the partial contribution of CYP3A4 to the metabolism of these two substrates as has been reported previously (Kajosaari et al., 2005; Cacabelos 2020).

A nonspecific CYP inhibitor (1 mM aminobenzotriazole) supplemented with a CYP2C9 inhibitor tienilic acid (15 μM), i.e., previously used as an application of the human hepatocyte relay method for fm estimation (Yang et al., 2016), inhibited depletion of the probe CYP substrates in long-term cocultured hepatocytes by up to 92% (CYP1A2), 0% (CYP2B6), 77% (CYP2C8), 51% (CYP2C9), 100% (CYP2C19), 96% (CYP2D6), and 83% (CYP3A4). This was aligned with the corresponding results when using the selective CYP inhibitors (Table 2). Further investigations of fm,CYP2B6 estimation in the current assay format were limited by the lack of available selective CYP2B6 substrates.

In Vitro Inhibition by Chemical Inhibitors of Non-P450 Enzyme Activities in the Liver. The chemical inhibitors furafylline (20 μM; CYP1A2), PPP (100 μM; CYP2B6), sulfaphenazole (100 μM; CYP2C9), NBPB (3 μM; CYP2C19), and quinidine (5 μM; CYP2D6) did not or only slightly inhibited formation of direct glucuronides of 17β-estradiol (10 μM) and zidovudine (10 μM) in incubations with recombinant human UGT1A1 and UGT2B7, respectively (Table 3). However, coincubation with 40 μM montelukast inhibited these isoforms by 96% and 65%, respectively. Also, itraconazole at 3 μM reduced the UGT1A1 marker activity by 62% with no impact on UGT2B7. At lower concentrations of 1 μM and 0.1 μM, respectively, montelukast and itraconazole did not significantly affect the UGT1A1 or 2B7 activities. This might reflect the incubation conditions as these molecules have extremely low fu(inc) values (montelukast: < 0.003 and itraconazole: 0.01) in the incubation medium supplemented with 10% FCS (Supplemental Fig. 1).

No inhibition effects of the inhibitors on recombinant human FMO3 activity (benzydamine oxidation) were exhibited. Metabolism of carbazeran (10 μM) was not affected by coincubation of the inhibitors using human liver cytosol, indicating no off-target activity of the chemical inhibitors on AO. In addition, no alteration of CLint for a SULT substrate troglitazone (10 μM) was observed in human liver cytosol supplemented with PAPS in the absence and presence of the CYP inhibitors except for 40 μM montelukast (CYP2C8 inhibitor). A lower concentration of montelukast (1 μM) did not inhibit CYP2C8.

In Vitro-In Vivo Extrapolation of fm,CYP3A4 for Reference Drugs. Values of fm,CYP3A4 of 13 drugs (all at 1 μM except for idasanutlin, which was at 10 μM), eliminated mainly by hepatic metabolism, were obtained by measuring the inhibitory effect of 3 μM itraconazole on the parent drug depletion during 4-days incubation in human long-term cocultured hepatocytes (Table 4). The selected drugs were mainly eliminated by hepatic metabolism without significant involvement of other elimination pathways such as urinary and biliary excretion. Therefore, the use of the reference fm,CYP3A4 estimated using the data from the clinical victim DDI studies (Ridtitid et al., 2005; Ohno et al., 2008; Cleary et al., 2018; Nemunaitis et al., 2018) was justified. Metabolic CLint of the reference compounds without inhibition effects were categorized from low (idasanutlin: 1.30 μl/min/mg) to high (nifedipine: > 200 μl/min/mg) according to the current measurement, and 7 drugs showed low to moderate intrinsic clearance in vitro (approximately < 10 μl/min/mg). Irrespective of the diverse drug dispositions with a various fm,CYP3A4 (Ohno et al., 2008), currently measured fm,CYP3A4 values estimated in this study were within 0.5- to 2-fold difference compared with the reference data of a number of drugs except for gefitinib, prednisolone, and simvastatin (Fig. 4).

Assuming negligible first pass effects, the statically predicted systemic exposure change of the reference 13 drugs with comedications of a strong CYP3A4 inhibitor was successfully categorized moderate/strong or moderate/weak victim DDI risk potential using the measured fm,CYP3A4 values, which were in line with those using the reference data (Table 4).

administration of drug compounds or media changes were made in this assay. The concentrations of the parent drug or selective metabolite on y-axis (μM) in semi-logarithmic scale were plotted against the incubation time on x-axis (day) except for (G). The profiles over time (mean, n = 2) were approximated according to linear regression analysis, resulting in calculation of the CLint values. Contribution of stromal cells (closed blue circles: with inhibition; open blue circles: without inhibition) was subtracted from the metabolic activity observed in the hepatocyte cocultures (closed red squares: with inhibition; open red squares: without inhibition), respectively. Limit of qualification values of the analytes are as follows: 0.42 nM for tacrine, 0.42 nM for bupropion, 2.54 nM for repaglinide, 2.66 nM for diclofenac, 6.82 nM for 4'-hydroxymephenytoin, 2.60 nM for dextromethorphan, and 0.40 nM for midazolam.

TABLE 3

Effects of chemical inhibitors on non-CYP enzyme marker activities

In vitro intrinsic metabolic clearance (CLint) values were determined by measuring linear depletion rates of the parent drugs (carbazeran and benzydamine at 10 μM, and troglitazone at 1 μM) or the subsequent metabolite formation (glucuronidated metabolite of 17β-estradiol at 1 μM and zidovudine at 10 μM) in i) recombinant UGTs supplemented with uridine 5′-diphosphoglucuronic acid, ii) recombinant FMO3 with NADPH, iii) human liver cytosols for AO, or iv) human liver cytosols with PAPS for SULTs (n = 1 or mean values of duplicate experiments). Fractions inhibited were calculated as [1 – (ratio of CLint in the presence versus absence of the chemical inhibitor)].

		Off-Target Inhibition of Selected Non-CYP Enzymes in Individual Enzyme Preparations or Liver Cytosols (Shown as Fraction Inhibited)				
	Chemical Inhibitor	UGT1A1(17β-estradiol)	UGT2B7(zidovudine)	FMO3(benzydamine)	AO(carbazeran)	SULT(troglitazone)
CYP1A2	furafylline (20 μM)	0.00	0.00	0.06	0.01	0.00
CYP2B6	PPP (100 μM)	0.00	0.14	0.00	0.03	0.04
CYP2C8	montelukast (1/40 μM)*a*	0.32/0.96	0.14/0.65	0.00	0.10	0.21/0.75
CYP2C9	sulfaphenazole (100 μM)	0.40	0.00	0.05	0.00	0.00
CYP2C19	NBPB (3 μM)	0.18	0.15	0.04	0.05	0.00
CYP2D6	quinidine (5 μM)	0.25	0.03	0.02	0.00	0.00
CYP3A4	Itraconazole (0.1/3 μM)[a]	0.00/0.62	0.00	0.11	0.00	0.02

[a]Inhibition effects of montelukast and itraconazole at lower concentrations (1 μM and 0.1 μM, respectively) besides high concentrations (40 μM and 3 μM, respectively) on UGT1A1 and UGT2B7 marker activities were incubated; otherwise only the effects of the inhibitors at high concentrations were investigated.

Discussion

Calculation of fm,CYP from the ratio of metabolic CLint in the presence and the absence of a chemical inhibitor in human hepatocytes or HLM is an established approach. However, the in vitro CLint can be difficult to determine precisely for low clearance compounds. In this study, chemical inhibition has been applied to long-term cocultured human hepatocytes and estimation of fm,CYP was thoroughly investigated for a set of drugs including those with low clearance. The HepatoPac coculture system is routinely used over an incubation period of 4 days without media exchange (Docci et al., 2020; Umehara et al., 2020). In the interest of achieving a simple assay format, depletion of the parent drug was pursued in this study without evaluation of metabolite formation except for 4'-hydroxymephenytoin formation (CYP2C19 marker activity).

As CYP3A4 is one of the major drug metabolizing enzymes and the victim DDI liability is of great concern for drug discovery and development, selection of the chemical inhibitor and optimization of the dosing concentration over the duration of incubation were carefully evaluated. By applying the measured total CLint values of the four CYP3A4 inhibitors (ketoconazole, ritonavir, itraconazole, and posaconazole) and assuming a linear one-compartment model, the unbound concentrations after dosing of these four inhibitors at total concentrations of 0.3, 1, and 3 μM to the assay samples were simulated. It was assumed that unbound concentrations of the inhibitor media supplemented with 10% FCS would represent concentration within the hepatocytes, neglecting any contributions of active transport. Unbound ketoconazole was rapidly depleted and was predicted to fall below the unbound reversible inhibition constant (Ki,u) (0.015 μM; SimCYP Version 18) at 24–48 hours (Fig. 3A). The respectively simulated unbound concentrations of itraconazole at an initial concentration of 3 μM were > 3-fold higher than a reported Ki,u of 0.001 μM (Chen et al., 2019a) (Fig. 3B). The metabolite hydroxyl-itraconazole might also additively contribute

TABLE 4

Estimated fm,CYP3A4 values in human long-term cocultured hepatocytes with the reference data among a number of CYP3A4 substrates

In vitro intrinsic metabolic clearance (CLint) values of 13 drugs were determined by measuring linear depletion rates of the parent drugs at 1 μM except for idasanutlin (10 μM) after incubating with human cocultured hepatocytes for 4 days in the absence and presence of the CYP3A4 inhibitor 3 μM itraconazole. CI95 represents the respective CLint with 95% interval for the fitting estimate of CLint based on the parent drug depletion profiles over time according to linear regression analysis. Based on these, CLint values of the fmCYP3A4 was estimated. The categories of victim DDI risks were given according to FDA (2020): no (AUCR < 1.25), weak (1.25 ≤ AUCR < 2), moderate (2 ≤ AUCR < 5), and strong (5 ≤ AUCR) using a static model predicted systemic exposure increase in the presence of strong CYP3A4 inhibition effects, representing the situation in a preclinical research and development setting where further information related to oral bioavailability and nonmetabolic clearance pathways are not yet available. Compounds classified into low–moderate CLint category without CYP3A4 inhibition (approximately < 3–10 μl/min/mg; Umehara et al., 2020*) were presented in bold. The data represent mean values of duplicate experiments. The reference fm,CYP3A4 data are taken from* Ohno et al., (2008) *based on clinical DDI data unless otherwise noted.*

Compounds	CLint w/o CYP3A4 Inhibition (μl/min/mg)	CLint with CYP3A4 Inhibition (μl/min/mg)	fm,CYP3A4[Measured]	Victim DDI Risk Using Measured fm,CYP3A4	fm,CYP3A4[Reference]	Victim DDI Risk Using Reference fm,CYP3A4
Alectinib	12.5 (CI95: 0.60)	5.3 (CI95: 0.20)	0.57	moderate	0.40[a]	weak
Alprazolam	3.14 (0.14)	0.50 (0.15)	0.84	strong	0.75	moderate
Atorvastatin	14.3 (0.26)	1.91 (0.17)	0.87	strong	0.68	moderate
Buspirone	60.8 (0.00)	8.35 (0.65)	0.86	strong	0.99	strong
Gefitinib	20.1 (1.70)	3.36 (0.32)	0.83	strong	0.39	weak
Idasanutlin	1.30 (0.3)	1.00 (0.40)	0.23	weak	0.25[b]	weak
Mefloquine	6.26 (0.32)	3.69 (0.13)	0.41	weak	0.47[c]	weak
Nifedipine	>200 (0.00)	6.93 (0.33)	0.99	strong	0.78	moderate
Prednisolone	37.0 (8.11)	13.2 (0.65)	0.64	moderate	0.18	no
Simvastatin	49.1 (4.17)	23.2 (5.03)	0.54	moderate	1.00	strong
Triazolam	26.9 (2.08)	1.65 (0.30)	0.94	strong	0.93	strong
Zolpidem	9.64 (0.39)	3.57 (0.32)	0.63	moderate	0.40	weak
Zopiclone	10.3 (0.82)	3.29 (0.27)	0.68	moderate	0.44	weak

N.C., not calculated.
[a]Cleary et al., (2018)
[b]Nemunaitis et al., (2018)
[c]Thai population (Ridtitid et al., 2005)

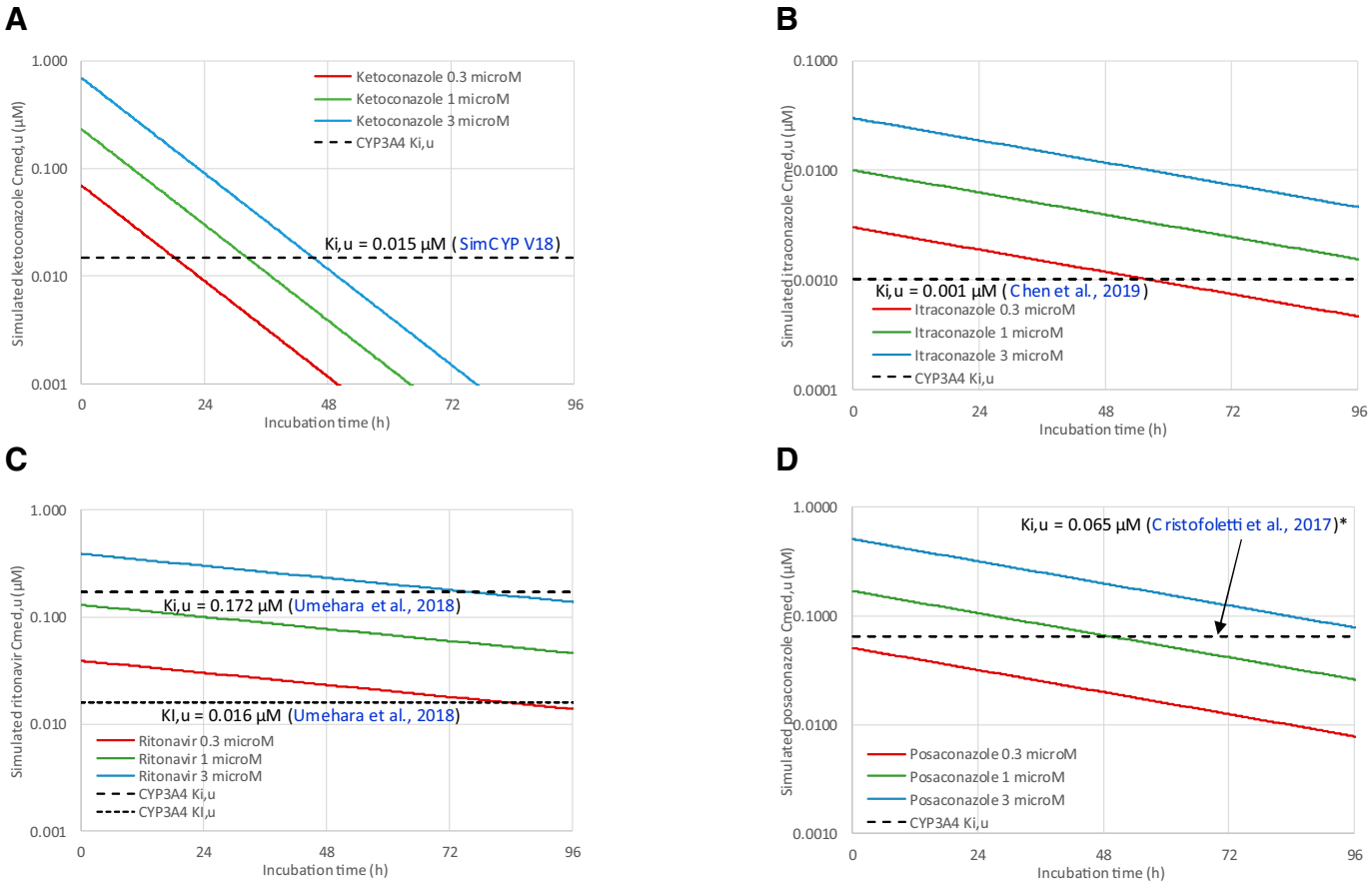

Fig. 3. Simulated unbound concentration profiles of CYP3A4 inhibitors over time in human long-term cocultured hepatocyte incubates. By applying the measured total CLint values of the four CYP3A4 inhibitors in cocultured hepatocytes [see *Results*; (A) ketoconazole (24.1 µl/min/mg), (B) itraconazole (6.50 µl/min/mg), (C) ritonavir (3.50 µl/min/mg), and (D) posaconazole (6.50 µl/min/mg)], the unbound concentrations after single dosing of the four inhibitors at total concentrations of 0.3, 1, and 3 µM to the incubates were simulated for 4 days. The simulated unbound concentration profiles were visually compared with the corresponding Ki,u or (unbound) concentration that results in half-maximal inactivation of enzymes (KI,u) in HLM shown as black dotted lines in each panel. Reported Ki,u values of ketoconazole, ritonavir, itraconazole, and posaconazole were 0.015 µM (SimCYP Version 18), 0.172 µM (Umehara et al., 2018), 0.001 µM (Chen et al., 2019a), and 0.065 µM (Cristofoletti et al., 2017), respectively. Ritonavir was the only compound out of the four inhibitors showing time-dependent inhibition of CYP3A4 with a KI,u of 0.016 µM (Umehara et al., 2018). *A reported lower value. A higher end of Ki,u (1.7 µM) would result in no inhibition potential of posaconazole on CYP3A4 in the in vitro assay setting.

to the net inhibition effect of itraconazole on CYP3A4 (Chen et al., 2019a). Despite the identical total CLint of posaconazole and itraconazole (6.50 µl/min/mg), only moderate inhibition effects of posaconazole on midazolam were observed (Table 1). This is likely due to the lower inhibitory potency of posaconazole. As illustrated in Fig. 3D, unbound posaconazole concentrations after single dosing on day 1 at 0.1, 1, or 3 µM (total) were close to or much below reported Ki,u values for CYP3A4 (0.065–1.7 µM; Cristofoletti et al., 2017) and dropped below effective inhibitory concentrations e.g., 20 x Ki,u during the first day of incubation.

The current chemical inhibition assay using cocultured human hepatocytes was successfully applied to 13 marketed drugs and provided reasonable fm,CYP3A4 values relative to the reference data except for gefitinib, simvastatin, and prednisolone (Table 4). Gefitinib is a dual substrate of CYP3A4 and CYP1A1, a highly variable and extra-hepatically expressed enzyme (Lang et al., 2019; Xu and Li, 2019). Therefore, hepatocytes without relevant expression of CYP1A1 might overestimate the CYP3A4 contribution to total metabolism. Thus, an fm,CYP3A4 of 0.83 is higher than determined in vivo (0.39) where CYP1A1 involvement was taken into account. Simvastatin fm,CYP3A4 in vitro (0.54) was greatly underestimated relative to the reference (1.00). However, DDI-PBPK modeling with an fm,CYP3A4 of 0.9–1.0 occasionally overestimated the effect of CYP3A4 inhibitors such as erythromycin and ketoconazole on the systemic exposure of simvastatin (SimCYP Version 20; model verification document); otherwise, conversion of simvastatin (lactone) to its acid form, besides the active uptake in liver, might impact characterization of this drug's disposition in vitro and in vivo. Although prednisolone is known to be a CYP3A4 substrate, the reported in vivo fm,CYP3A4 value was only 0.18, notably lower than the value of 0.64 estimated in this study. A report of a 2-fold increase in prednisolone exposure when coadministered with hormone contraceptives (University of Washington Drug Interaction Database: https://didb.druginteractionsolutions.org/) is also suggestive of a higher in vivo fm value, perhaps more aligned with our in vitro estimate. Hence, irrespective of clearance classification, the fm,CYP3A4 values could be now calculated with high resolution and complemented the standard enzymology assay using HLM and recombinant CYP enzymes at preclinical stage. Involvement of extra-hepatic metabolism, renal, and fecal excretion to total clearance is also critical to assess the victim DDI liability.

The chemical inhibitors of CYP1A2 (furafylline, 20 µM), CYP2C8 (montelukast, 40 µM), CYP2C19 (NBPB, 3 µM), CYP2D6 (quinidine, 5 µM), and CYP3A4 (itraconazole, 3 µM) inhibited their respective depletion of the probe substrates by up to 93%, 82%, 83%, 88%, and 83%–88%, respectively (Tables 1 and 2). Regarding the inhibition of CYP1A2, CYP2C19, CYP2D6, and CYP3A4, the nominal inhibitor concentrations at time 0 were equivalent or 2-fold higher compared

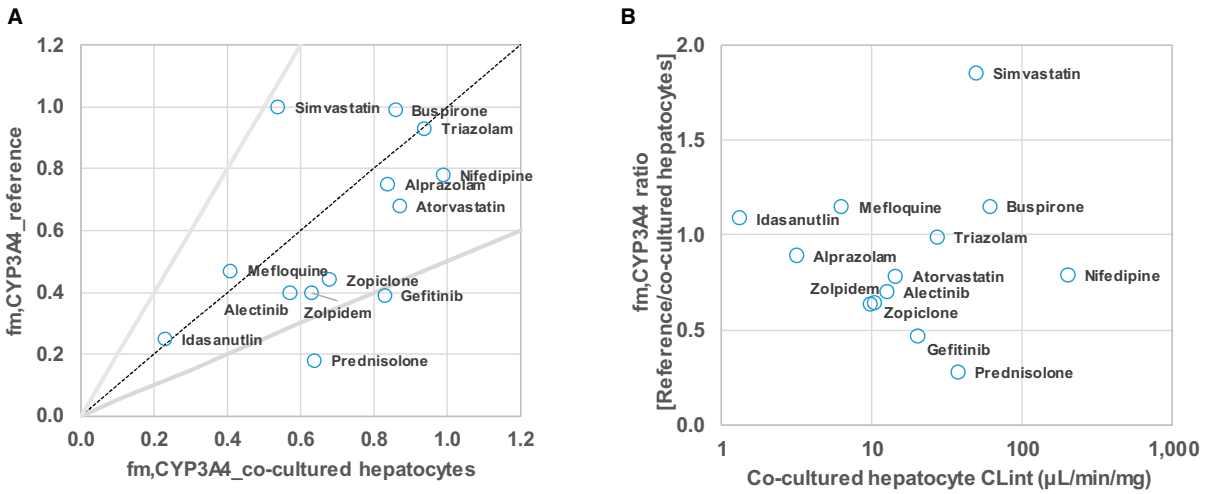

Fig. 4. Comparison of fm,CYP3A4 values in human long-term cocultured hepatocytes with the reference data among a number of CYP3A4 substrates. (A) fm,CYP3A4 estimated in vitro in human cocultured hepatocytes by incubating 13 CYP3A4 substrates with low to high clearance classification in the absence and presence of 3 µM itraconazole compared with the clinical reference data as summarized in Table 4. The solid lines represent 0.5- and 2-fold ranges of the line of unity (broken line). (B) Differences between measured and reference values shown as a ratio plotted against the respective in vitro CLint in the absence of inhibition effects.

with the standard chemical inhibition study using HLM (Cai et al., 2004; Walsky and Obach, 2007; Njuguna et al., 2016). On the contrary, a 20-fold higher concentration of montelukast (40 µM) in the cocultured hepatocyte incubation than HLM (2 µM) was deployed to achieve sufficient marker activity inhibition. The different inhibitor concentrations in the two systems could be derived from protein abundance in the incubation. Provided an extremely low fu(inc) of montelukast in the hepatocyte media samples (< 0.003) with 10% FCS, a lowest unbound concentration after initial incubation with montelukast at 20 µM was approximately estimated to be < 0.12 µM, which could reach the Ki,u in HLM (0.007–0.18 µM) indicating the sufficient inhibition of CYP2C8 (Supplemental Fig. 1). However, this might not be accomplished if a low montelukast concentration at 2 µM as used in HLM was applied initially. Along the line, the lowest unbound concentrations of furafylline in the human hepatocyte cocultures were > 10-fold higher than the Ki,u (Supplemental Fig. 1). Quinidine unbound concentration on day 4 (~0.111 µM) similar with or below the Ki,u in HLM (0.019–0.931 µM) still provided the sufficient inhibition on the CYP2D6 marker activity (Supplemental Fig. 1; Table 2).

37% Inhibition of sulfaphenazole (40 µM) on diclofenac metabolism as the CYP2C9 marker activity (Table 2) was completely aligned with the respective fraction clearance in vivo. Diclofenac was metabolized by hepatic CYP2C9, hepatic/renal UGT2B7 followed by renal excretion with corresponding fractions of 0.29, 0.64, and 0.07, respectively (SimCYP Version 16; model verification document). No off-target activity of sulfaphenazole at a high concentration 100 µM on UGT2B7 was also confirmed in this study (Table 3). McGinnity et al. (2006) demonstrated the long-term knockdown of CYP2C9 by tienilic acid in plated hepatocytes and a good estimation of fm,CYP2C9. Effective inhibition of tolbutamide turnover (a CYP2C9 probe substrate) was reported on coincubation of tienilic acid at an extremely low concentration 0.015 µM using human cocultured hepatocytes without supplementation of protein in the media (Smith et al., 2021). Hence, tienilic acid can be used as a mechanism-based CYP2C9 inhibitor in place of the competitive inhibitor sulfaphenazole. Estimation of fm,CYPs using time-dependent inhibitors will work and can benefit from it to characterizing a competition between enzyme inactivation and de novo synthesis of CYP enzymes (Fowler and Zhang, 2008).

Due to reliability of fm,CYP3A4 estimation within 2-fold of the reference data for 10 out of the 13 CYP3A4 substrates tested in this study (Fig. 4; Table 4), fmCYP3A4 ≥ 0.5 representing moderate to sensitive victim DDI risk (AUC ratio ≥ 2) in systemic circulation with comedication of a strong CYP3A4 inhibitor can be flagged with confidence even for low clearance drug candidates (FDA, 2020). An identical concept can be applied to other CYP enzymes, and this and other studies have shown the feasibility to extend the methodology. Validation of the approach for other CYP enzymes using multiple drug examples with in vivo fm data will be needed to build confidence in the approach for these enzymes as well as for CYP3A4.

In conclusion, the successful use of 3 µM itraconazole to estimate fm,CYP3A4 by coincubating with the test drug candidate in long-term of pooled human hepatocytes was demonstrated effective in vitro-in vivo extrapolation of fm,CYP3A4 values. The CYP enzyme reaction phenotyping method could be further applied for other CYP enzymes (CYP1A2, CYP2C8, CYP2C9, CYP2C19, CYP2D6) using the inhibitors: 20 µM furafulline, 40 µM montelukast, 40 µM sulfaphenazole, 3 µM NBPB, and 5 µM quinidine, respectively. Qualification of the chemical inhibition assay lies in selecting chemical inhibitors retaining sufficient unbound concentrations in the samples over an extended incubation time period.

These assay capabilities are extremely useful for drug discovery and development of a drug candidate in terms of victim DDI assessment together with running the respective PBPK modeling. The new fm estimation methodology using long-term hepatocyte cultures and selective inhibition of individual CYP metabolism pathways offers a substantial opportunity to estimate fm of moderate clearance drug candidates at an earlier stage in drug development, before detailed knowledge of metabolism products has been gained and before metabolite standards and radiolabeled drug substance are available. The method is also significantly resource-sparing since only a few experiments need to be run using a standardized experimental protocol and only requiring an analytical method for the drug candidate itself.

Authorship Contributions

Participated in research design: Klammers, Ekiciler, Umehara.
Conducted experiments: Klammers, Goetschi, Ekiciler, Walter.
Performed data analysis: Klammers, Goetschi, Walter, Umehara.
Wrote or contributed to the writing of the manuscript: Klammers, Parrott, Fowler, Umehara.

References

Bohnert T, Patel A, Templeton I, Chen Y, Lu C, Lai G, Leung L, Tse S, Einolf HJ, Wang YH, et al.; International Consortium for Innovation and Quality in Pharmaceutical Development (IQ) Victim Drug-Drug Interactions Working Group (2016) Evaluation of a new molecular entity as a victim of metabolic drug-drug interactions-an industry perspective. *Drug Metab Dispos* **44**:1399–1423.

Cacabelos R (2020) Pharmacogenetic considerations when prescribing cholinesterase inhibitors for the treatment of Alzheimer's disease. *Expert Opin Drug Metab Toxicol* **16**:673–701.

Cai X, Wang RW, Edom RW, Evans DC, Shou M, Rodrigues AD, Liu W, Dean DC, and Baillie TA (2004) Validation of (-)-N-3-benzyl-phenobarbital as a selective inhibitor of CYP2C19 in human liver microsomes. *Drug Metab Dispos* **32**:584–586.

Chan TS, Yu H, Moore A, Khetani SR, and Tweedie D (2019) Meeting the challenge of predicting hepatic clearance of compounds slowly metabolized by cytochrome P450 using a novel hepatocyte model, HepatoPac. *Drug Metab Dispos* **47**:58–66.

Chan TS, Scaringella YS, Raymond K, and Taub ME (2020) Evaluation of erythromycin as a tool to assess CYP3A contribution of low clearance compounds in a long-term hepatocyte culture. *Drug Metab Dispos* **48**:690–697.

Chen Y, Cabalu TD, Callegari E, Einolf H, Liu L, Parrott N, Peters SA, Schuck E, Sharma P, Tracey H, et al. (2019) Recommendations for the design of clinical drug-drug interaction studies with itraconazole using a mechanistic physiologically-based pharmacokinetic model. *CPT Pharmacometrics Syst Pharmacol* **8**:685–695.

Chen YC, Kenny JR, Wright M, Hop CECA, and Yan Z (2019) Improving confidence in the determination of free fraction for highly bound drugs using bidirectional equilibrium dialysis. *J Pharm Sci* **108**:1296–1302.

Cleary Y, Gertz M, Morcos PN, Yu L, Youdim K, Phipps A, Fowler S, and Parrott N (2018) Model-based assessments of CYP-mediated drug-drug interaction risk of alectinib: physiologically based pharmacokinetic modeling supported clinical development. *Clin Pharmacol Ther* **104**:505–514.

Cristofoletti R, Patel N, and Dressman JB (2017) Assessment of bioequivalence of weak base formulations under various dosing conditions using physiologically based pharmacokinetic simulations in virtual populations. case examples: ketoconazole and posaconazole. *J Pharm Sci* **106**:560–569.

Docci L, Parrott N, Krähenbühl S, and Fowler S (2019) Application of new cellular and microphysiological systems to drug metabolism optimization and their positioning respective to in silico tools. *SLAS Discov* **24**:523–536.

Docci L, Klammers F, Ekiciler A, Molitor B, Umehara K, Walter I, Krähenbühl S, Parrott N, and Fowler S (2020) In vitro to in vivo extrapolation of metabolic clearance for UGT substrates using short-term suspension and long-term co-cultured human hepatocytes. *AAPS J* **22**:131.

Fowler S and Zhang H (2008) In vitro evaluation of reversible and irreversible cytochrome P450 inhibition: current status on methodologies and their utility for predicting drug-drug interactions. *AAPS J* **10**:410–424.

Greenblatt DJ and Harmatz JS (2015) Ritonavir is the best alternative to ketoconazole as an index inhibitor of cytochrome P450-3A in drug-drug interaction studies. *Br J Clin Pharmacol* **80**:342–350.

Harper TW and Brassil PJ (2008) Reaction phenotyping: current industry efforts to identify enzymes responsible for metabolizing drug candidates. *AAPS J* **10**:200–207.

Hultman Ia, Vedin C, Abrahamsson A, Winiwarter S, and Darnell M (2016) Use of HμREL human coculture system for prediction of intrinsic clearance and metabolite formation for slowly metabolized compounds. *Mol Pharm* **13**:2796–2807.

Huth F, Gardin A, Umehara K, and He H (2019) Prediction of the impact of cytochrome P450 2C9 genotypes on the drug-drug interaction potential of siponimod with physiologically-based pharmacokinetic modeling: a comprehensive approach for drug label recommendations. *Clin Pharmacol Ther* **106**:1113–1124.

Kajosaari LI, Laitila J, Neuvonen PJ, and Backman JT (2005) Metabolism of repaglinide by CYP2C8 and CYP3A4 in vitro: effect of fibrates and rifampicin. *Basic Clin Pharmacol Toxicol* **97**:249–256.

Khetani SR and Bhatia SN (2008) Microscale culture of human liver cells for drug development. *Nat Biotechnol* **26**:120–126.

Kratochwil NA, Meille C, Fowler S, Klammers F, Ekiciler A, Molitor B, Simon S, Walter I, McGinnis C, Walther J, et al. (2017) Metabolic profiling of human long-term liver models and hepatic clearance predictions from in vitro data using nonlinear mixed-effects modeling. *AAPS J* **19**:534–550.

Lang D, Radtke M, and Bairlein M (2019) Highly variable expression of CYP1A1 in human liver and impact on pharmacokinetics of riociguat and granisetron in humans. *Chem Res Toxicol* **32**:1115–1122.

McGinnity DF, Berry AJ, Kenny JR, Grime K, and Riley RJ (2006) Evaluation of time-dependent cytochrome P450 inhibition using cultured human hepatocytes. *Drug Metab Dispos* **34**:1291–1300.

Murgasova R (2019) Further assessment of the relay hepatocyte assay for determination of intrinsic clearance of slowly metabolised compounds using radioactivity monitoring and LC-MS methods. *Eur J Drug Metab Pharmacokinet* **44**:817–826.

Nemunaitis J, Young A, Ejadi S, Miller W, Chen LC, Nichols G, Blotner S, Vazvaei F, Zhi J, and Razak A (2018) Effects of posaconazole (a strong CYP3A4 inhibitor), two new tablet formulations, and food on the pharmacokinetics of idasanutlin, an MDM2 antagonist, in patients with advanced solid tumors. *Cancer Chemother Pharmacol* **81**:529–537.

Njuguna NM, Umehara KI, Huth F, Schiller H, Chibale K, and Camenisch G (2016) Improvement of the chemical inhibition phenotyping assay by cross-reactivity correction. *Drug Metab Pers Ther* **31**:221–228.

Ohno Y, Hisaka A, Ueno M, and Suzuki H (2008) General framework for the prediction of oral drug interactions caused by CYP3A4 induction from in vivo information. *Clin Pharmacokinet* **47**:669–680.

Ridtitid W, Wongnawa M, Mahatthanatrakul W, Raungsri N, and Sunbhanich M (2005) Ketoconazole increases plasma concentrations of antimalarial mefloquine in healthy human volunteers. *J Clin Pharm Ther* **30**:285–290.

Smith S, Lyman M, Ma B, Tweedie D, and Menzel K (2021) Reaction phenotyping of low-turnover compounds in long-term hepatocyte cultures through persistent selective inhibition of cytochromes P450. *Drug Metab Dispos* **49**:995–1002.

Schumacher H, Hoffmann S, Holmboe C, and Møller JK (2001) A procedure for evaluation and documentation of susceptibility test methods using the susceptibility of Klebsiella pneumoniae to ciprofloxacin as a model. *J Antimicrob Chemother* **48**:493–500.

Umehara KI, Huth F, Won CS, Heimbach T, and He H (2018) Verification of a physiologically based pharmacokinetic model of ritonavir to estimate drug-drug interaction potential of CYP3A4 substrates. *Biopharm Drug Dispos* **39**:152–163.

Umehara K, Cantrill C, Wittwer MB, Di Lenarda E, Klammers F, Ekiciler A, Parrott N, Fowler S, and Ullah M (2020) Application of the extended clearance classification system (ECCS) in drug discovery and development: selection of appropriate in vitro tools and clearance prediction. *Drug Metab Dispos* **48**:849–860.

Walsky RL and Obach RS (2007) A comparison of 2-phenyl-2-(1-piperidinyl)propane (ppp), 1,1′,1′′-phosphinothioylidynetrisaziridine (thioTEPA), clopidogrel, and ticlopidine as selective inactivators of human cytochrome P450 2B6. *Drug Metab Dispos* **35**:2053–2059.

Yang X, Atkinson K, and Di L (2016) Novel cytochrome P450 reaction phenotyping for low-clearance compounds using the hepatocyte relay method. *Drug Metab Dispos* **44**:460–465.

Xu ZY and Li JL (2019) Comparative review of drug-drug interactions with epidermal growth factor receptor tyrosine kinase inhibitors for the treatment of non-small-cell lung cancer. *Onco-Targets Ther* **12**:5467–5484.

de Zwart L, Snoeys J, De Jong J, Sukbuntherng J, Mannaert E, and Monshouwer M (2016) Ibrutinib dosing strategies based on interaction potential of CYP3A4 perpetrators using physiologically based pharmacokinetic modeling. *Clin Pharmacol Ther* **100**:548–557.

Address correspondence to: Dr. Kenichi Umehara, Roche Pharmaceutical Research and Early Development, Grenzacherstrasse 124, CH-4070 Basel, Switzerland. E-mail: kenichi.umehara@roche.com

DMD-AR-2021-000765: supplementary information

Journal:

Drug Metabolism and Disposition

Article:

Estimation of fraction metabolized by cytochrome P450 (CYP) enzymes using long-term co-cultured human hepatocytes

Florian Klammers, Andreas Goetschi, Aynur Ekiciler, Isabelle Walter, Neil Parrott, Stephen Fowler, Kenichi Umehara

Roche Pharmaceutical Research and Early Development, Roche Innovation Center, Grenzacherstrasse 124, CH-4070 Basel, Switzerland (F.K., A.G., A.E., I.W., N.P., S.F., K.U.)

Supplementary Figure S1: Representative depletion profiles of CYP inhibitors over time in human HepatoPac®.

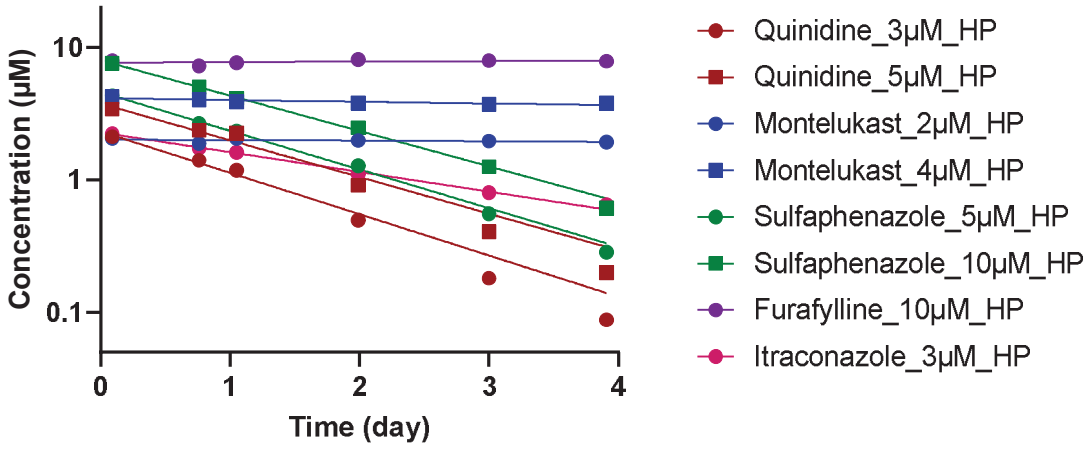

Chemical inhibitors on CYP1A2 (furafylline; 10 µM), CYP2C8 (montelukast; 2 and 4 µM), CYP2C9 (sulfaphenazole; 5 and 10 µM), CYP2D6 (quinidine; 3 and 5 µM) and CYP3A4 (itraconazole; 3 µM) were administered at time 0 on the day 1, and then incubated for four days in human hepatocytes co-cultured with mouse stromal cells. The compound concentrations on y-axis (µM) in semi-logarithmic scale were plotted against the incubation time on x-axis (day).

Supplementary Figure S2: In vitro CLint variability of a control CYP3A4 substrate quinidine in human HepatoPac® since October 2016